British Geological Survey
NATURAL ENVIRONMENT RESEARCH COUNCIL

The Response of Compact Bentonite during a 1-D Gas Flow Test

Minerals & Waste Programme

Open Report OR/17/067

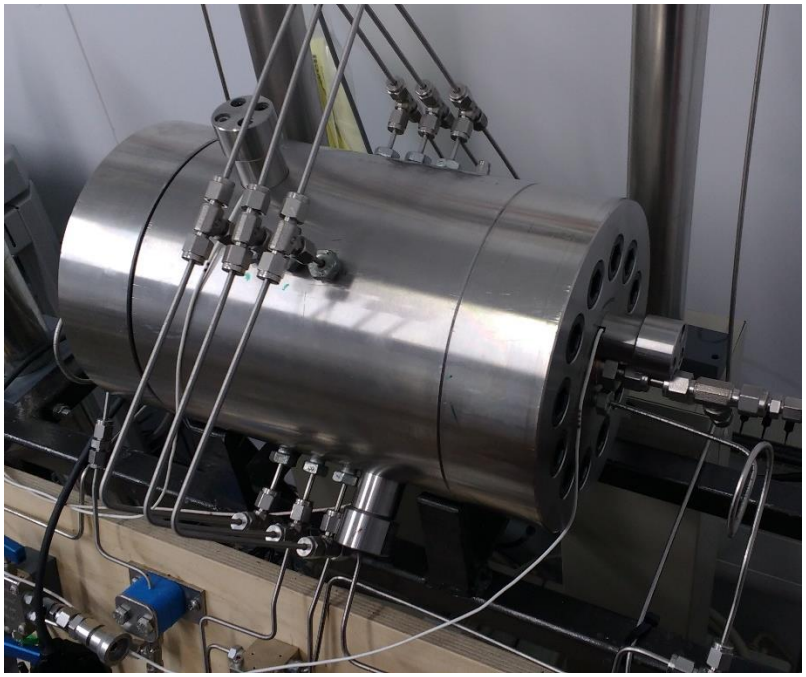

BRITISH GEOLOGICAL SURVEY

DECOVALEX PROGRAMME

OPEN REPORT OR/17/067

The Response of Compact Bentonite during a 1-D Gas Flow Test

K.A. Daniels, J.F. Harrington

Contributor/editor

R.J. Cuss

Keywords

Report; Compact Bentonite; Gas Flow; Stress Response; Permeability.

Front cover

Cover picture details, The custom-built 1-D experimental apparatus.

Bibliographical reference

DANIELS, K A, HARRINGTON, J F, 2017. The Response of Compact Bentonite during a 1D Gas Flow Test. *British Geological Survey Open Report*, OR/17/067. 22pp.

Keyworth, Nottingham British Geological Survey 2017

BRITISH GEOLOGICAL SURVEY

The full range of our publications is available from BGS shops at Nottingham, Edinburgh, London and Cardiff (Welsh publications only) see contact details below or shop online at www.geologyshop.com

The London Information Office also maintains a reference collection of BGS publications, including maps, for consultation.

We publish an annual catalogue of our maps and other publications; this catalogue is available online or from any of the BGS shops.

The British Geological Survey carries out the geological survey of Great Britain and Northern Ireland (the latter as an agency service for the government of Northern Ireland), and of the surrounding continental shelf, as well as basic research projects. It also undertakes programmes of technical aid in geology in developing countries.

The British Geological Survey is a component body of the Natural Environment Research Council.

British Geological Survey offices

BGS Central Enquiries Desk

Tel 0115 936 3143 Fax 0115 936 3276
email enquiries@bgs.ac.uk

Environmental Science Centre, Keyworth, Nottingham NG12 5GG

Tel 0115 936 3241 Fax 0115 936 3488
email sales@bgs.ac.uk

The Lyell Centre, Research Avenue South, Edinburgh EH14 4AP

Tel 0131 667 1000 Fax 0131 668 2683
email scotsales@bgs.ac.uk

Natural History Museum, Cromwell Road, London SW7 5BD

Tel 020 7589 4090 Fax 020 7584 8270
Tel 020 7942 5344/45 email bgslondon@bgs.ac.uk

Cardiff University, Main Building, Park Place, Cardiff CF10 3AT

Tel 029 2167 4280 Fax 029 2052 1963

Maclean Building, Crowmarsh Gifford, Wallingford OX10 8BB

Tel 01491 838800 Fax 01491 692345

Geological Survey of Northern Ireland, Department of Enterprise, Trade & Investment, Dundonald House, Upper Newtownards Road, Ballymiscaw, Belfast, BT4 3SB

Tel 028 9038 8462 Fax 028 9038 8461
www.bgs.ac.uk/gsni/

Parent Body

Natural Environment Research Council, Polaris House, North Star Avenue, Swindon SN2 1EU

Tel 01793 411500 Fax 01793 411501
www.nerc.ac.uk

Website www.bgs.ac.uk
Shop online at www.geologyshop.com

Foreword

This report is the published product of a study by the British Geological Survey (BGS) undertaken as part of the DECOVALEX-2019 programme of work. The study contributes to Task A: modElliNg Gas INjection ExpERiments (ENGINEER) of the programme. The authors would like to thank Humphrey Wallis and Wayne Leman for the construction of the apparatus used for the experimental testing, and Neil Stacey for the preparation of the sample used. Robert Cuss is thanked for his review of this report. Caroline Graham and Andrew Wiseall are thanked for their technical discussions and support of this research.

Contents

Foreword ..... **i**

Contents ..... **i**

Summary ..... **iv**

1 Introduction **4**

2 Experimental Approach **5**

2.1 Sample Preparation 5

2.2 Method 6

2.3 Sample Hydration: 9

3 Gas testing **11**

3.1 Before Gas Breakthrough 11

3.2 Gas breakthrough, steady state and shut-in behaviour 13

4 Summary **17**

References **17**

FIGURES

Figure 1: Post-test X-Ray images of the sample [A] oriented parallel to vertical and [B] and oriented parallel to horizontal. The apparent deviation of the end faces of the cylinder from horizontal is an optical artefact of the X-Ray image. The small circular depression of the material in the end face at the base of the image was created by the pushrod leading to the injection-end axial load cell. 5

Figure 2: The experimental apparatus and sample assembly 6

Figure 3: Above: Cut-away diagram of the pressure vessel showing the apparatus components and instrumentation. Below: image of the sample showing the relative positions of the load cells and pore pressure filters. 8

Figure 4: A simplified schematic diagram showing the fluid pathway and connections between the syringe pumps, interface vessels (IVs) and the sample assembly in the pressure vessel. The instrumentation of the vessel (porewater pressure transducers and axial and radial load cells) is not shown. The IV on the left contains the helium, which is topped up through the valve at the top of the vessel. The valves are represented by circles. 8

Figure 5: Swelling pressure measured by the axial and radial load cells, injection pressure and backpressure. 9

Figure 6: Axial and radial porewater pressure for the first 40 days. The small deviation in the radial porewater data between days 8-11 was due to using the incorrect pump set point and was quickly rectified. 11

Figure 7: Porewater pressures up to gas entry at 63 days. 12

Figure 8: A 3 MPa gas pressure was applied at the injection end of the sample. The flow rate was set to 500 μL/h and the swelling pressures remained constant. At day 54, the injection pump was refilled with DI water and the flow rate was reduced to 375 μL/h. The injection system (pump and IV) was refilled again at day 61. At this point, 60.13 ml of DI water was drawn back from the IV into the pump and the IV was refilled with helium at a gas pressure of 8715 kPa. Gas entry occurred at day 63. 12

Figure 9: [A] Injection pressure, backpressure and radial porewater pressure transducer data from day 61 to day 75. [B] Stress measured on the 3 radial and two axial load cells (dashed lines) from day 61 to day 75. Injection pressure (red line) inflow (dark green line and outflow (light green line) are shown over the same time interval. The increase in outflow at 63.8 days signifies gas breakthrough. 14

Figure 10: [A] Injection pressure, backpressure and radial porewater pressure transducer data from day 61 to day 121. [B] Swelling pressure (stress) measured on the 3 radial and two axial load cells (dashed lines) from day 61 to day 121. Injection pressure (red line) inflow (dark green line and outflow (light green line) are shown over the same time interval. The increase in outflow at 63.8 days signifies gas breakthrough. 15

Figure 11: [A] Temperature and pressure data from the injection pump and the 5 load cells for the complete gas stage. Minor fluctuations in the load cell data correspond with small changes in temperature, however the temperature has not affected the trends observed in the test. [B] Temperature and flow rate data over the same time interval. 16

TABLES

Table 1: Sample dimensions and geotechnical parameters to 2 decimal places. The length, diameter and weight were each measured three times and were then averaged. 5

Table 2: Relative positions of load cells and porewater pressure filters. Axial distance is to the centre point of each sensor. Angular rotation is anti-clockwise with the zenith taken vertically at the top of the vessel at the radial load cell 1 position (see also Figure 3). Radial porewater sensors 1 to 4 comprise radial porewater array 1, radial sensors 5 to 8 form radial porewater array 2 and radial porewater array 3 comprises radial sensors 9 to 12..... 7

Table 3: Dates and pump volumes recording the addition of helium to the left-hand IV, water added to the injection pump, or gas removed from the backpressure pump. 10

Summary

This report describes the results of a 1-D gas injection test on compact Mx80 bentonite. The test comprises the first dataset for Stage 1A of Task A of the DECOVALEX-2019 programme, which has been designed to improve our understanding of the migration of repository gases through clay-based materials.

Over the duration of the testing period, pressurised helium gas was applied to the face of the injection end of the clay sample, and the gas pressure was increased until the entry pressure was exceeded and gas entered the sample. The gas then migrated through the clay and changes in porewater pressure, swelling pressure and flowrate were observed by the instrumentation around the sample. Gas breakthrough occurred as outflow was recorded by the backpressure pump that corresponded with the changes in pressure. The data presented in this study shows that dynamic processes operate within the clay causing differing responses to be recorded on the monitoring instruments. The recorded response of the clay highlights the spatial and temporal development of permeability within the clay sample over the duration of the test.

1 Introduction

Clay-based engineered barriers are a vital part of the design concept for the geological disposal of radioactive waste. The corrosion of metallic canister materials in the subsurface in anoxic conditions, as could occur in the KBS-3 disposal concept, radiolysis of water and radioactive decay of the waste could all cause the production of gas. The accurate understanding of the processes governing the movement of repository gases through engineered barriers is therefore of importance in understanding their long-term performance and integrity. The migration of gas through the engineered barrier may occur either by diffusion alone or a combination of advection and diffusion. If the gas production rate is greater than the diffusion rate through the material, gas will accumulate as a free phase (Weetjens and Sillen, 2006; Ortiz *et al.*, 2002; Wikramaratna *et al.*, 1993) and the pressure will rise until the gas can advect through the material. The advection of gas will be influenced by the layout of the radioactive waste repository, therefore a consideration of the advection of gas in a repository will have an impact on both its design and layout.

Recent work has shown that plastic clays, such as bentonite, idealised two-phase flow through a porous medium often does not adequately explain experimental observations (Horseman *et al.*, 1996, 2004; Harrington and Horseman, 1999; Angeli *et al.*, 2009; Harrington *et al.*, 2009). Further work is required to understand such processes as gas entry, gas breakthrough, gas flow, flow path homogeneity and pathway sealing, as well as the dilatant mechanisms in the clay that control them. In addition, the gas permeability is likely to be a time- and location-dependent variable rather than a material property because it relies on the quantity, size and connectivity of pressure-induced pathways through the material (Horseman and Harrington, 1997). It is also unclear what effect previous gas flow through a clay will have on any subsequent gas flow; the first incidence of gas flow may reduce the effectiveness of the barrier against further gas migration.

Task A of the DECOVALEX-2019 programme has been designed to address these questions, and to improve understanding of the advection of repository gases through clay-based materials. A 1-D gas injection test performed on compact Mx80 bentonite has been conducted at the British Geological Survey. This test represents the first test dataset for Stage 1A of the DECOVALEX Task A; the results of this experiment are presented in this report.

2 Experimental Approach

2.1 SAMPLE PREPARATION

A 1-D gas injection test has been conducted on a sample of pre-compacted Mx80 bentonite supplied by Clay Technology AB (Lund, Sweden). The bentonite had dry and bulk densities of 1.56 kg/m^3 and 1.99 kg/m^3 respectively (Table 1). The pre-compacted bentonite was cut into a cylinder using a machine lathe yielding an accurately dimensioned sample that formed a snug fit with the internal bore of the testing apparatus; the length of the cylindrical sample was cut parallel to the compaction direction. The sample was machine lathed without cutting lubrication and care was taken to minimise moisture loss by keeping the sample wrapped in plastic packaging wherever and whenever possible. A hole at the midplane of the sample with a diameter of 6.35 mm was drilled from the backpressure end of the sample to a depth of 64.8 mm, to allow a stainless steel tube with a filter at its tip to be inserted into the sample (providing a static measure of gas pressure during testing). The hole at the midplane was also drilled using the machine lathe at 200 rpm; the drill bit did not clog and no heat was able to build up in the clay during the drilling of the hole. The sample was stored in vacuum-sealed packaging when not in use and the sample dimensions and weight were recorded prior to testing. X-ray radiography was used to image the fabric of the bentonite before the sample was installed into the experimental apparatus and once the test had concluded and the sample had been removed from the rig (**Figure 1**).

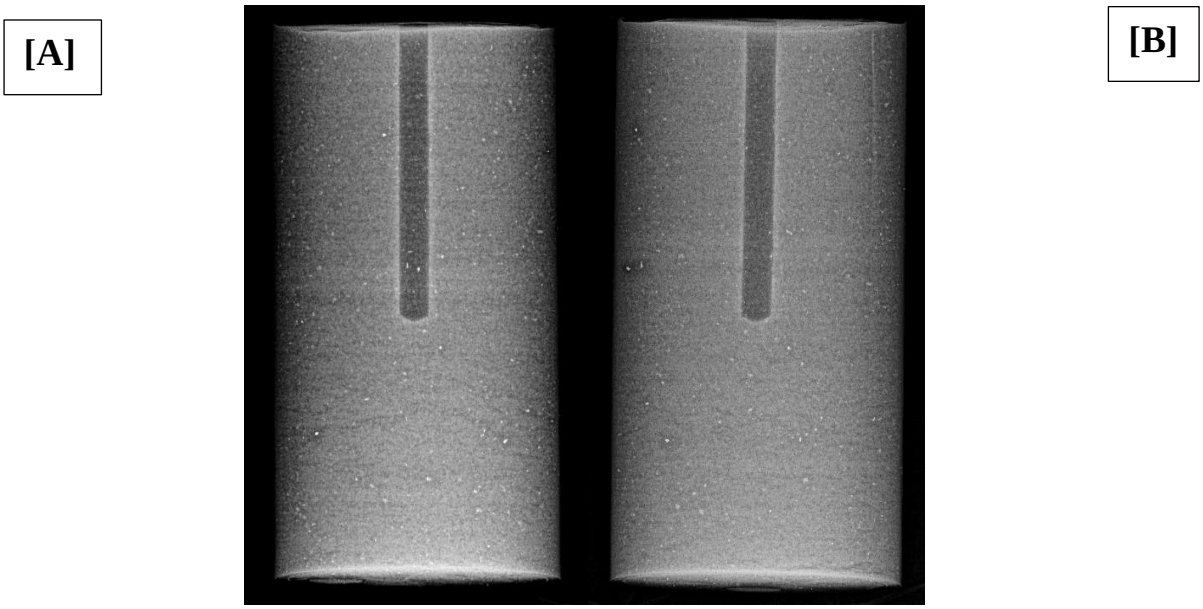

Figure 1: Post-test X-Ray images of the sample [A] oriented parallel to vertical and [B] and oriented parallel to horizontal. The apparent deviation of the end faces of the cylinder from horizontal is an optical artefact of the X-Ray image. The small circular depression of the material in the end face at the base of the image was created by the pushrod leading to the injection-end axial load cell.

	Length (mm)	Diameter (mm)	Weight (g)	Dry Density (kg/m^3)	Bulk Density (kg/m^3)
Sample Mx80D	119.88	59.59	671.65	1.56	1.99

Table 1: Sample dimensions and geotechnical parameters to 2 decimal places. The length, diameter and weight were each measured three times and were then averaged.

2.2 METHOD

2.2.1 Apparatus

A constant volume pressure vessel, comprising a custom-built hollow 316 stainless steel cylinder and two detachable end-closures, was used for the testing (Figure 2). The pressure vessel was instrumented with 2 axial and 3 radial load cells, as well as 3 radial arrays of 4 porewater pressure transducers that were positioned regularly around the circumference of the vessel. The name, position and measurement type of each instrument used in this test are detailed in Table 2 and Figure 3. De-ionised water (DI) was used as the permeant to hydrate the sample prior to gas testing, and subsequently, as the backpressure fluid during the gas test. Helium was used as the permeant. The fluids were supplied to the sample through sintered stainless steel filters with a 3mm thickness, positioned at each end of the sample and over the ports to the porewater pressure transducers.

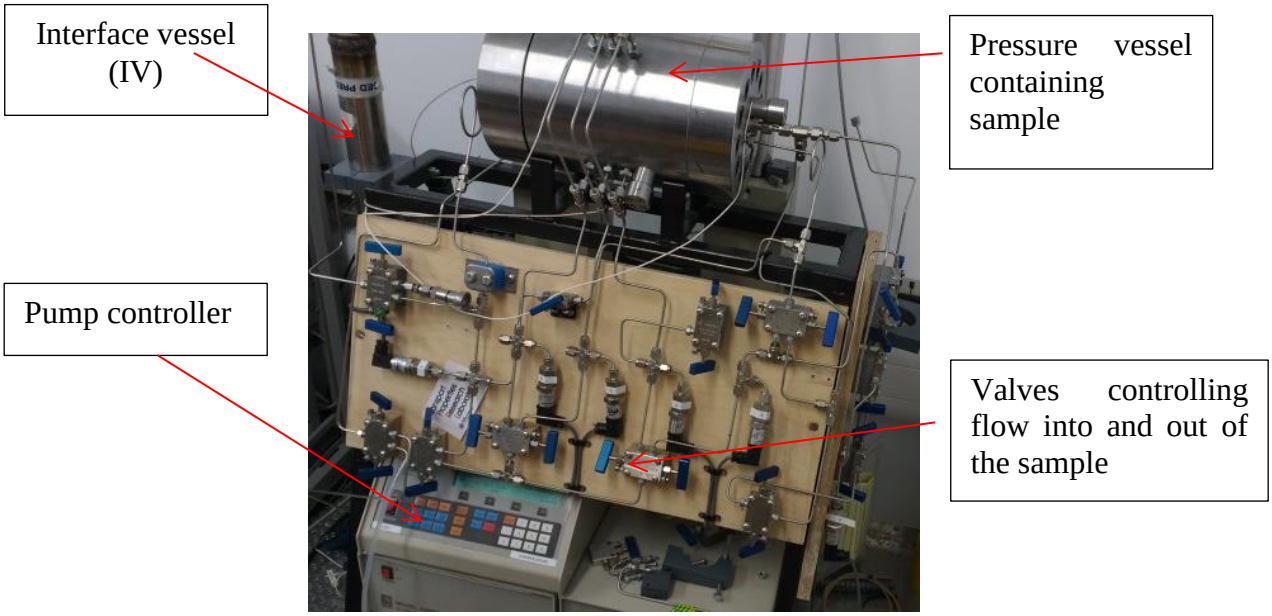

Figure 2: The experimental apparatus and sample assembly

2.2.2 Procedure

Before installing the sample, the radial filters (Table 2), connecting stainless steel tubing and the backpressure filter were flushed with DI to remove any air from the system. The injection filter was maintained dry to prevent water from entering the injection side of the sample ahead of the gas during the gas testing. The sample was slotted into the pressure vessel, the end-closures were fitted and the tubing was connected. The injection axial load cell housing was loosened before the injection end-closure was fitted so ensure that the pushrod between the clay and the load cell remained free-moving. The caphead screws on the backpressure end-closure were tightened first and to their maximum extent so that the end-closure was flush with the body of the vessel. The caphead screws on the injection end-closure were subsequently tightened to an approximate torque of 8 Nm, resulting in a gap of 1.89 mm between the end-closure and the vessel body and the application of an initial pre-stress on the axial faces of the sample of 3127 kPa (injection) and 5145 kPa (backpressure). These pre-stresses dropped to 2566 kPa and 3680 kPa respectively before increasing again as the clay hydrated.

Array	Sensor name	Axial distance from backpressure face (mm)	Rotation around bore of vessel (degrees)
Axial stress	Injection load cell	120	90
Radial stress	Radial load cell 1	104.8	0
Radial stress	Radial load cell 2	60	120
Radial stress	Radial load cell 3	15.2	240
Axial stress	Backpressure load cell	0	30
Radial porewater array 1	Radial 1	81.4	330
	Radial 2	81.4	60
	Radial 3	81.4	150
	Radial 4	81.4	240
Radial porewater array2	Radial 5	60	330
	Radial 6	60	60
	Radial 7	60	150
	Radial 8	60	240
Radial porewater array 3	Radial 9	38.6	330
	Radial 10	38.6	60
	Radial 11	38.6	150
	Radial 12	38.6	240
Midplane filter	Middle	60	0

Table 2: Relative positions of load cells and porewater pressure filters. Axial distance is to the centre point of each sensor. Angular rotation is anti-clockwise with the zenith taken vertically at the top of the vessel at the radial load cell 1 position (see also Figure 3). Radial porewater sensors 1 to 4 comprise radial porewater array 1, radial sensors 5 to 8 form radial porewater array 2 and radial porewater array 3 comprises radial sensors 9 to 12.

Volumetric flow rates were controlled or monitored using a pair of Teledyne ISCO-100DM, Series D, syringe pumps operated from a single digital control unit. The position of each pump piston was determined by an optically encoded disc graduated in segments equivalent to a change in volume of 4.825 nL. Movement of the pump piston was controlled by a microprocessor, which continuously monitored and adjusted the rate of rotation of the encoded disc using a DC-motor connected to the piston assembly via a geared worm drive. This allowed each pump to operate in either constant pressure or constant flow modes. A programme written in LabVIEW^{TM} elicited data from the pump at pre-set time intervals. Testing was performed in an air-conditioned laboratory at a nominal temperature of 20 ºC ±2 °C.

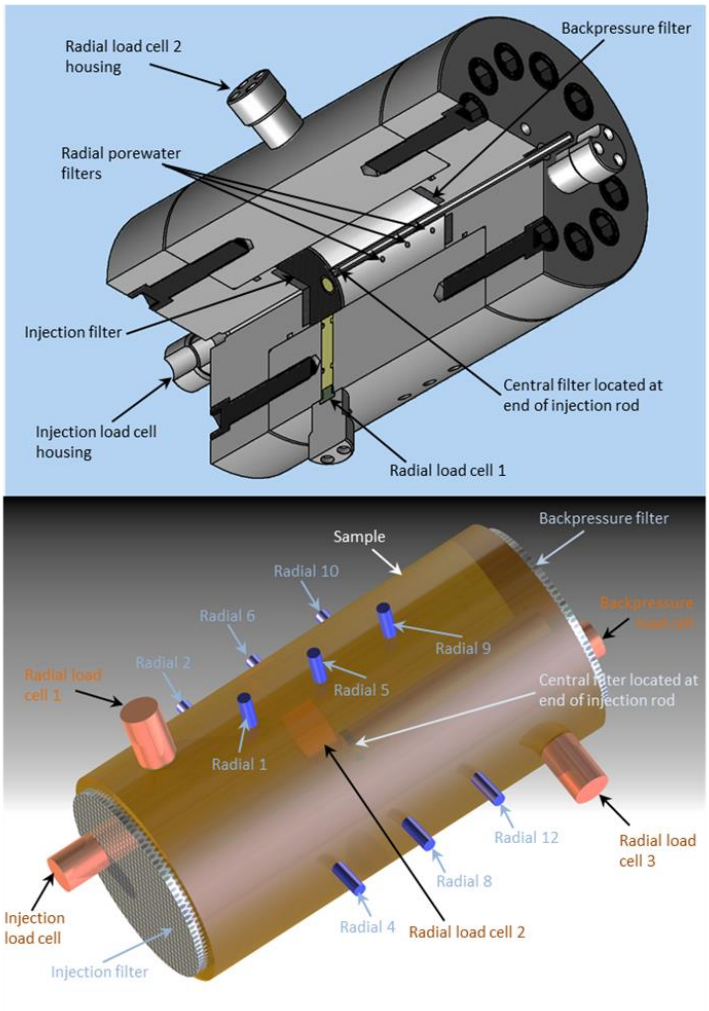

Figure 3: Above: Cut-away diagram of the pressure vessel showing the apparatus components and instrumentation. Below: image of the sample showing the relative positions of the load cells and pore pressure filters. Figure from Harrington and Tamayo-Mas, 2016.

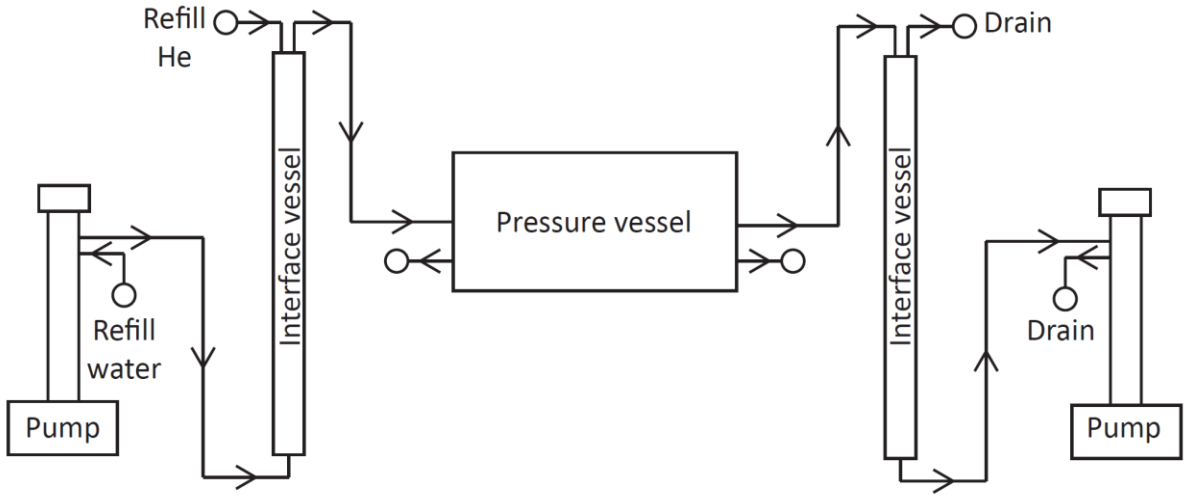

Figure 4: A simplified schematic diagram showing the fluid pathway and connections between the syringe pumps, interface vessels (IVs) and the sample assembly in the pressure vessel. The instrumentation of the vessel (porewater pressure transducers and axial and radial load cells) is not shown. The IV on the left contains the helium, which is topped up through the valve at the top of the vessel. The valves are represented by circles.

Helium was supplied to the sample from an interface vessel (IV) located between the ISCO pump and injection face of the sample (**Figure 4**). To compress and displace the gas, water from the ISCO pump was injected into the base of the IV. In this way, the gas was water saturated and thus would not have a drying effect on the clay and the gas pressure could be increased or controlled depending on the needs of the test. The test comprised two stages: hydration of the sample (Stage 1) followed by gas testing (Stage 2). After gas breakthrough and a period of gas flow through the sample, the injection pump was stopped whilst the swelling pressures (stresses) and porewater pressures were continuously monitored. The test ran for a duration of 265 days.

2.3 SAMPLE HYDRATION:

After installation, the sample was allowed to equilibrate with the water in the radial filters and backpressure end-closure filter for a period of 7.3 days. There was no air in these filters; the injection filter however was dry and no water was present in the tubes to the midplane filter. At the start of the test, the porewater pressure was at atmospheric pressure. During this hydration, the porewater pressure in each array and axial backpressure filter was monitored (Figure 5), as was the development of the swelling pressure (Figure 6).

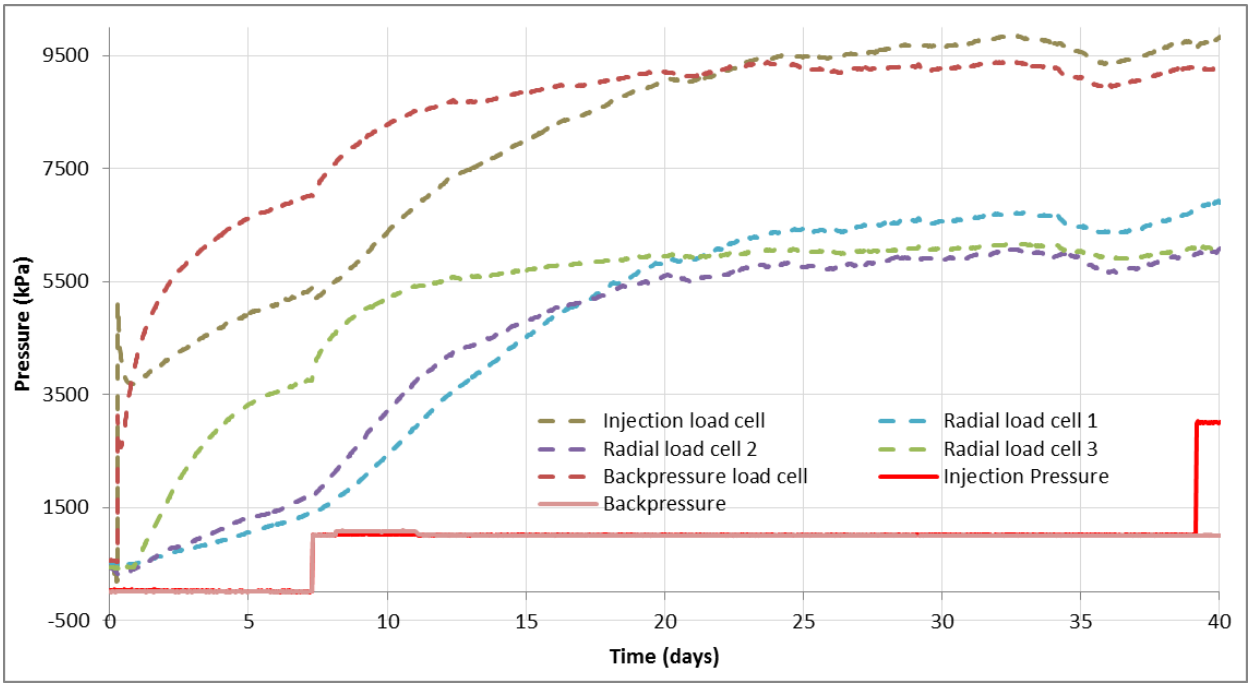

Figure 5: Swelling pressure measured by the axial and radial load cells, injection pressure and backpressure.

At day 7.3 active hydration of the sample began by pressurisation of the backpressure and radial filter arrays using DI water. To this end, the backpressure pump was initially set to 500 kPa. Next, the 3 radial arrays were pressurised using the backpressure pump, while a helium gas pressure of 1 MPa was generated in the injection filter (using the injection pump). Backpressure in the axial and radial arrays was then increased over the space of 2 minutes in 100 kPa steps to 1 MPa. The sample was allowed to hydrate for the following 32 days (Figure 5 and Figure 6). The gas pressure in the injection filter was maintained constant at 1000 kPa to prevent water ingress from the hydration systems into the injection filter.

Date	Test Day	Pump Volume Before	Pump Volume After	Comment
10/03/16	0	47.97 ml		Pump A starting volume
10/03/16	0	102.99 ml		Pump B starting volume
17/03/16	7	300 ml		Starting IV volume of He at 845 kPa
17/03/16	7	102.99 ml	49.72 ml	Pump B vol. decrease to raise IV He pressure to 1000 kPa
18/04/16	39	20.45 ml	101.42 ml	IV refilled with He at 3000 kPa
03/05/16	54	6.25 ml	102.15 ml	Pump A refilled with water
10/05/16	61	40.75 ml	100.88 ml	IV refilled with He at 8715 kPa
10/05/16	61	34.8 ml	6.58 ml	Pump B drained
16/05/16		85 ml	14 ml	Pump B drained
17/05/16		72.7 ml	9.7 ml	Pump B drained
17/05/16		40 ml	11.7 ml	Pump B drained
18/05/16		71 ml	9.5 ml	Pump B drained
18/05/16		39 ml	9.1 ml	Pump B drained
19/05/16		70.9 ml	8.9 ml	Pump B drained
19/05/16		40 ml	6.8 ml	Pump B drained
20/05/16		71.3 ml	7.2 ml	Pump B drained
27/06/16		89.40 ml	25.76 ml	Pump B drained

Table 3: Dates and pump volumes recording the addition of helium to the left-hand IV, water added to the injection pump, or gas removed from the backpressure pump.

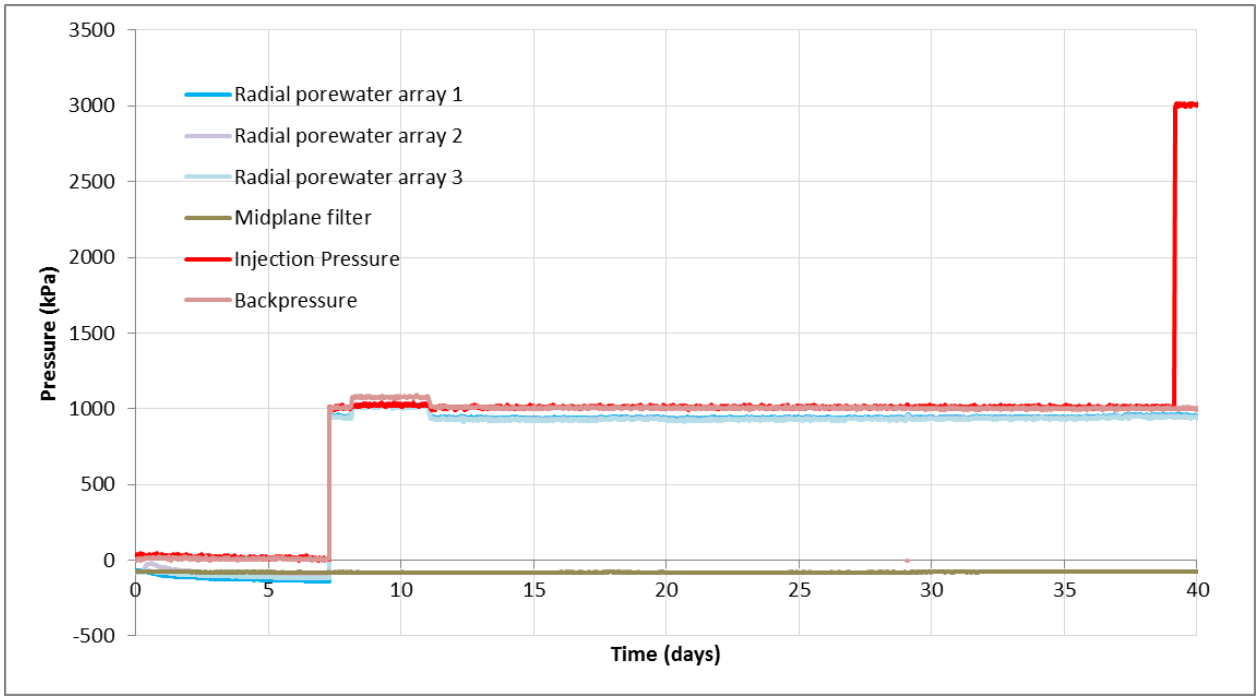

Figure 6: Axial and radial porewater pressure for the first 40 days. The small deviation in the radial porewater data between days 8-11 was due to using the incorrect pump set point and was quickly rectified.

3 Gas testing

3.1 BEFORE GAS BREAKTHROUGH

Gas testing began on day 39. Additional helium was added to the IV to increase pressure to 3 MPa (Table 3). Gas pressure was then held constant for a further 7 days to allow the system to equilibrate with the DI water in the IV. At day 46, the injection pump was set to a constant flow rate of 500 μL/h. The injection pressure gradually increased for the next 8 days from 3 MPa to 5 MPa whilst the volume of fluid in the injection pump decreased from 102.7 ml to 6.25 ml. Data from the axial and radial load cells and the porewater pressure sensors is presented in Figure 7 and Figure 8. At day 54, the DI water in the injection pump was refilled by 95.9 ml to 102.15 ml and the flow rate was reduced to 375 μL/h to create a consistent ramp of pressure following an increase in volume (see Figure 8).

At day 46, as the gas pressure ramp was initiated, and the pressure registered by the transducer attached to the injection end-closure filter showed an immediate increase in pressure (Figure 7). This is in contrast to the radial porewater pressures, which initially decreased, and in the case of arrays 1 and 2, then slowly increased again. The midplane porewater filter however, showed no obvious change between the start of gas testing and gas breakthrough; its value remained just below zero for the whole of this first part of the test. Althoughnot able to measure an accurate value of suction, the small negative values demonstrate that there is a suction at this point with water being drawn from the filter into the clay. Detailed inspection of the data in Figure 7 shows that the porewater pressure in radial array 1, closest to the injection end of the sample, increased most quickly as gas breakthrough approached. The cause for this rise is unclear and may relate to a hydrodynamic effect as the gas acted against the injection face of the clay. In contrast, the rate of change in porewater pressure of radial array 3, closest to the backpressure end of the sample, showed a steady decrease between days 46 and 61, followed by a slight increase until gas breakthrough, indicating that the sample was not in hydraulic equilibrium at the start of gas testing.

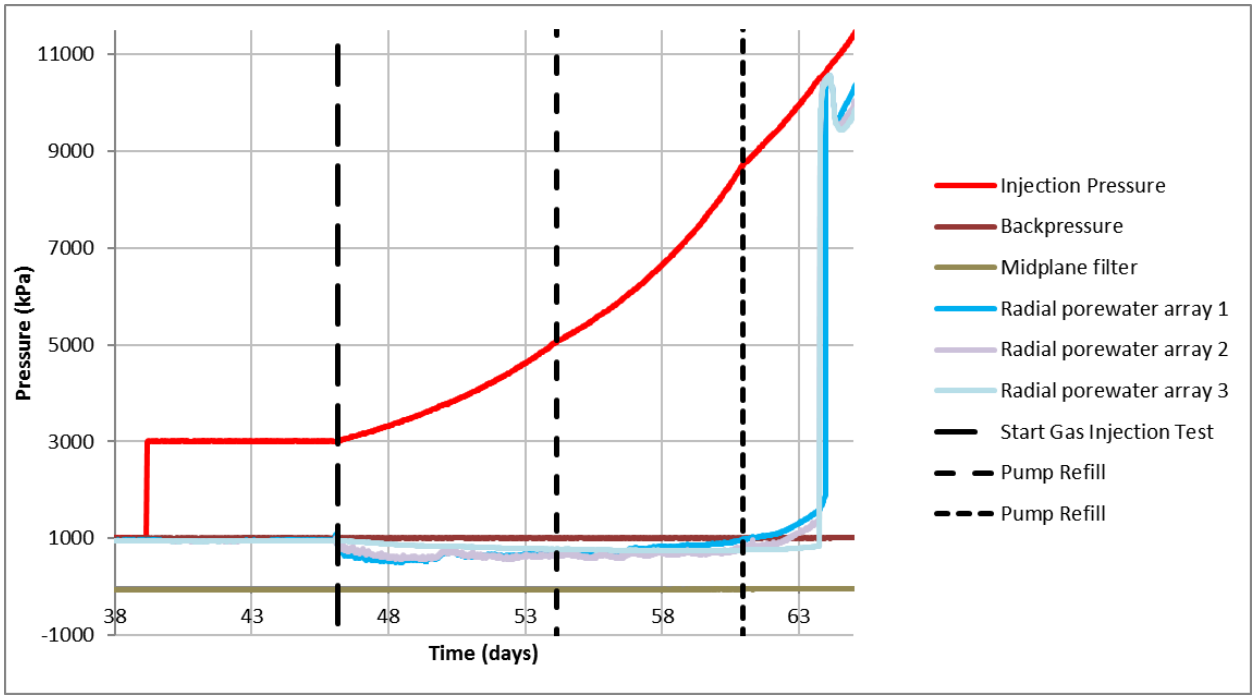

Figure 7: Porewater pressures up to gas entry at 63 days.

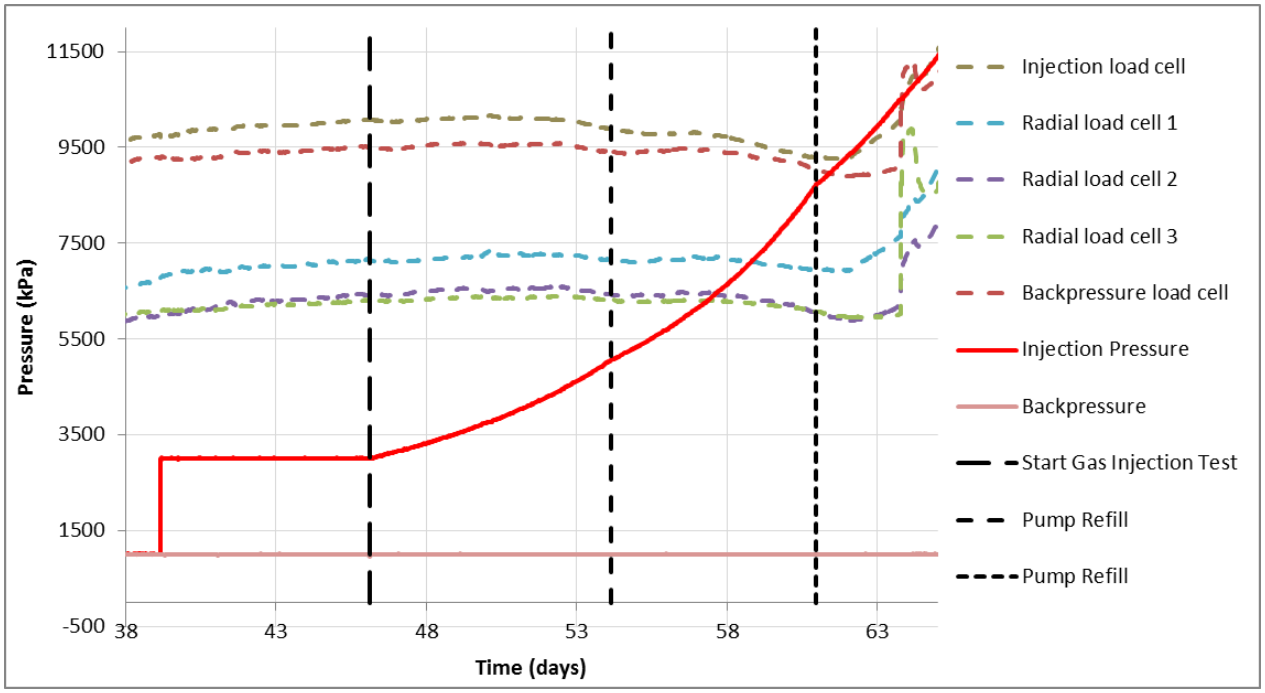

Figure 8: A 3 MPa gas pressure was applied at the injection end of the sample. The flow rate was set to 500 µL/h and the swelling pressures remained constant. At day 54, the injection pump was refilled with DI water and the flow rate was reduced to 375 µL/h. The injection system (pump and IV) was refilled again at day 61. At this point, 60.13 ml of DI water was drawn back from the IV into the pump and the IV was refilled with helium at a gas pressure of 8715 kPa. Gas entry occurred at day 63.

At day 61, further helium was added to the IV to ensure there would be sufficient gas to complete the experiment (Table 3). This was done before the pressure in the injection filter reached the breakthrough pressure and gas started to flow through the sample; after breakthrough, it would not have been possible to provide additional helium to the IV without disrupting the flow of gas

through the sample. Therefore, at day 61, just before gas breakthrough occurred, approximately an additional 0.21 mol helium gas was added to the IV, causing the injection pump volume to increase from 40.75 ml to 100.88 ml (Table 3).

3.2 GAS ENTRY, GAS BREAKTHROUGH AND SHUT-IN BEHAVIOUR

Gas entry occurred at 63 days, and the injection pressure at this point was 10.5 MPa. After gas entry, the porewater pressure in arrays 2 and 3 rose sharply to a value close to the injection gas pressure (Figure 9 [A] and Figure 10 [A]). Interestingly, despite beginning to increase first, the increase in pressure in radial array 1 (closest to the injection face) lagged behind that of the other two arrays by just over 0.2 days, which could indicate that the gas flow was non-uniform. Alternatively, the gas pathway may have carried gas to the edge of the sample, pressurising arrays 2 and 3 more quickly. After a small drop in porewater pressure around day 64.5 (Figure 7 and Figure 9 [A]), porewater pressures then generally tracked the gas pressure for the following 11 days, with small deviations in the pressure traces probably reflecting changes in the stability, aperture and/or configuration of the pathways. At day 71, the injection pump was stopped. Between day 71 and day 76, the injection pressure decreased very slightly, whilst the porewater pressures decreased substantially (Figure 10 [A]) with porewater pressure in radial array 1 continuing to fall until day 81.

Examination of the axial and radial load cell data during gas entry and breakthrough (Figure 9 [B] and Figure 10 [B]) indicates that the swelling pressure (stress) within the sample increased at the same time as gas breakthrough was occurring in the backpressure filter. The largest increase in radial stress was observed in load cell 3. This, supported by the porewater pressure data above, indicates a rapid increase in porewater pressure around this location in the sample. Following gas breakthrough, the system approached a quasi-steady state as gas pressure tended towards an asymptote and flow out of the sample more closely matched the gas flow into the sample (Figure 9 [B]). The outflow reached a level that was just lower than the inflow, and it is possible that this discrepancy could have been caused by a very slight leakage. The continued increase in the stresses measured by the axial and radial load cells after the gas breakthrough event had occurred, mirroring the increase in injection pressure, suggested that the sample was not in complete hydraulic equilibrium at the start of the test and a redistribution of the fluid in the sample caused the clay to continue to expand.

At day 79, the injection pressure began to reduce at a slightly faster rate than it had been between days 71 and 79, the pressure in the three radial porewater pressure arrays and at the midplane started to increase again. This may suggest that another breakthrough event to the filter array was occurring. Alternatively, the increase in pressure measured by the midplane filter may be an artefact of the starting test conditions. If a filter is full of water, when gas reaches it at pressure an instant change in the pressure is observed, whilst if a filter is full of air, more gas is required at that filter to change the pressure. Radial filters 1-3 were filled with water at the start of the test, whilst the midplane filter was filled with air. Gas may therefore have been reaching the midplane filter since day 63 but the change in pressure recorded at that location would have been initially very small. Thereafter, the porewater pressure traces from each radial array continued to track the injection pressure response.

The dip in porewater pressure between days 71 and 81 also corresponded with a dip in swelling pressure and a reduction in outflow to zero (Figure 10 [B]). Radial load cell 3 shows a decrease in pressure most clearly over this time interval. This event appears to occur close to the cessation of pumping. However, by day 81, porewater pressures had rebounded suggesting the cessation of pumping was not the cause for the spontaneous change in porewater pressure.

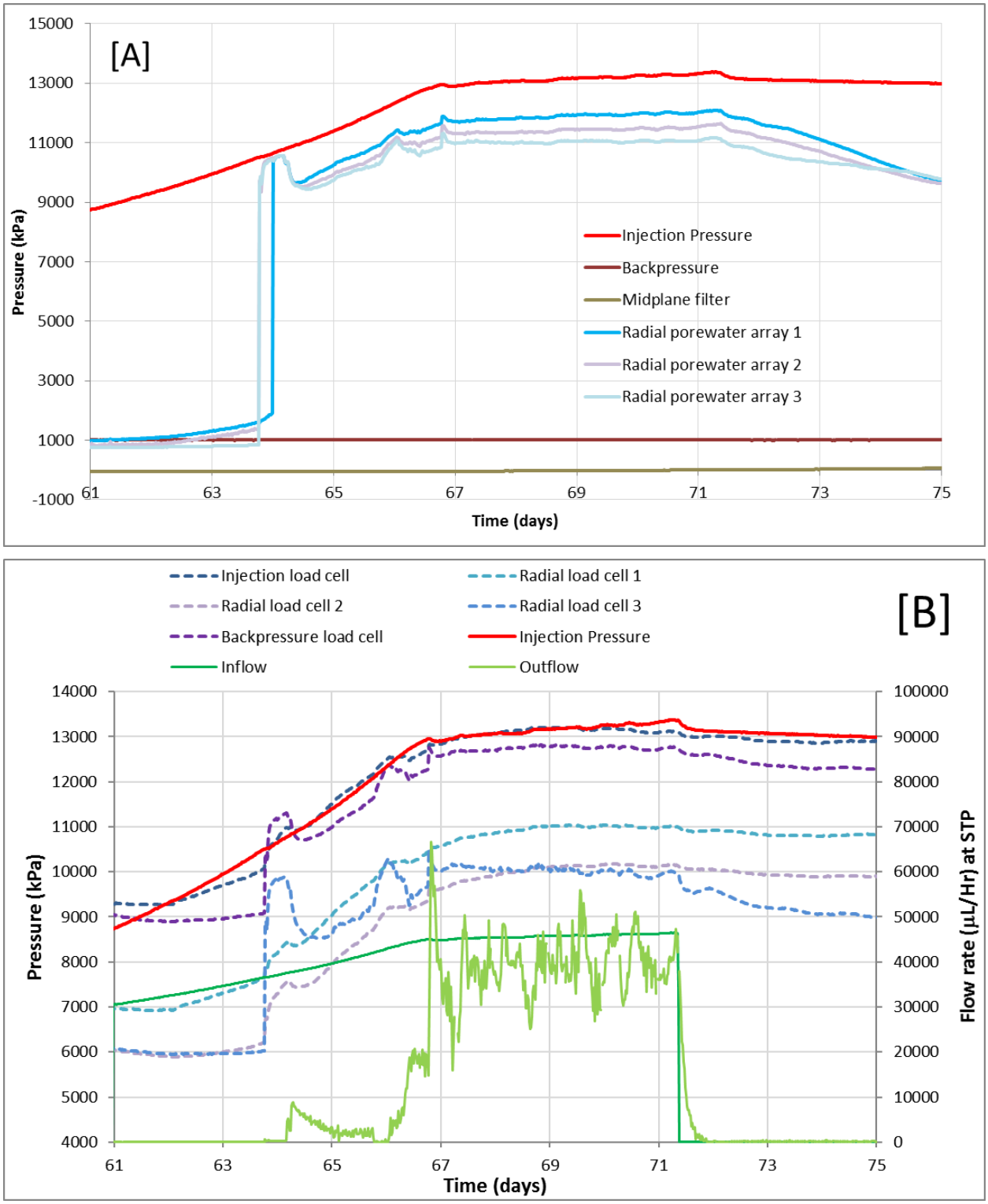

Figure 9: [A] Injection pressure, backpressure and radial porewater pressure transducer data from day 61 to day 75. [B] Stress measured on the 3 radial and two axial load cells (dashed lines) from day 61 to day 75. Injection pressure (red line) inflow (dark green line and outflow (light green line) are shown over the same time interval. The increase in outflow at 63.8 days signifies gas breakthrough.

Following gas breakthrough, the stress measured by the load cells and the porewater pressure transducers appeared to be integrally linked to the gas pressure within the clay; both the stress and outflow show a similar form as the gas pressure (Figure 9), which was not the case prior to breakthrough. This continued following the cessation of pumping, as gas pressure, porewater

pressure (Figure 10 [A]) and swelling pressure (Figure 10 [B]) began to decay. After day 81, the outflow was sporadic with positive fluctuations and spikes, despite the continued reduction in the injection pressure, suggesting new gas pathways continued to open and close. Some of these outflow events correlated with observed changes in the swelling pressure and porewater pressure, while others did not. The fluctuations in outflow are not related to changes in temperature (Figure 11). This suggests a dynamic process was operating within the clay, governing the local development of permeability.

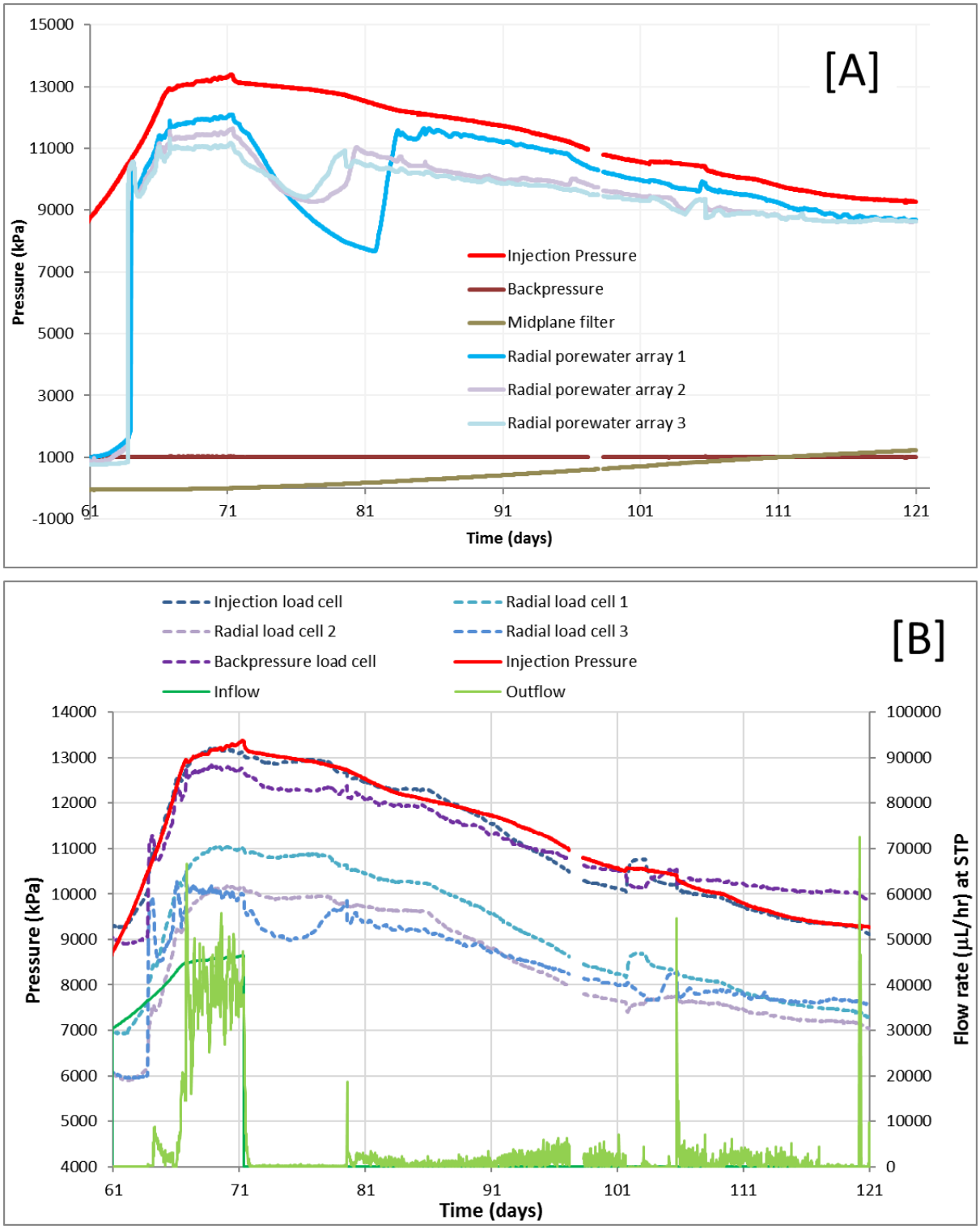

Figure 10: [A] Injection pressure, backpressure and radial porewater pressure transducer data from day 61 to day 121. [B] Swelling pressure (stress) measured on the 3 radial and two axial load cells (dashed lines) from day 61 to day 121. Injection pressure (red line) inflow

(dark green line and outflow (light green line) are shown over the same time interval. The increase in outflow at 63.8 days signifies gas breakthrough.

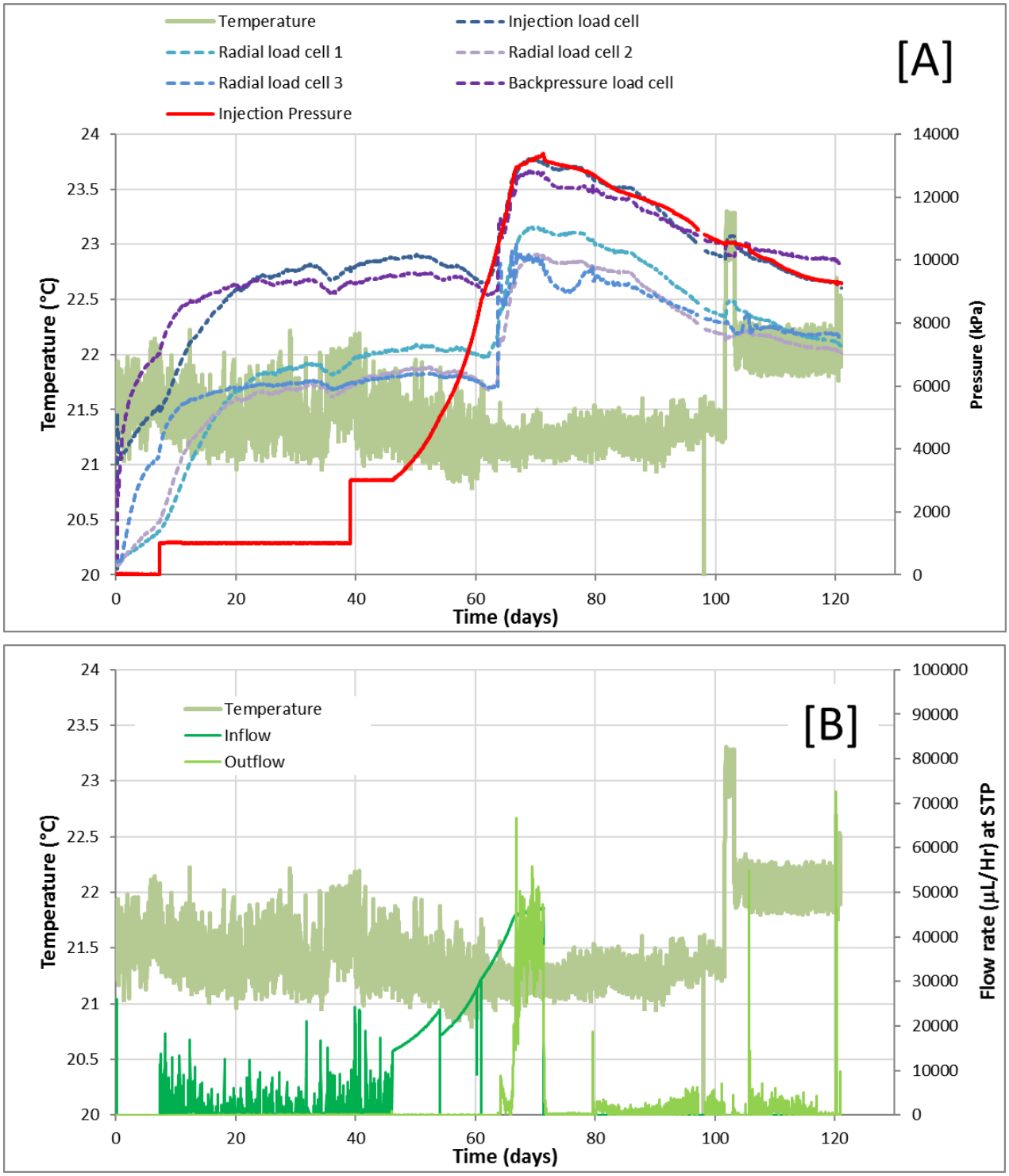

Figure 11: [A] Temperature and pressure data from the injection pump and the 5 load cells for the complete gas stage. Minor fluctuations in the load cell data correspond with small changes in temperature, however the temperature has not affected the trends observed in the test. [B] Temperature and flow rate data over the same time interval.

4 Summary

A 1-D gas injection test on compact Mx80 bentonite has been conducted and the results have been presented. The test has comprised two stages: an initial hydration of the sample with DI water from the backpressure end, and a gas-testing phase. The hydration was conducted at 1 MPa, with a helium pressure of the same magnitude applied to the injection end of the sample to prevent the injection filter from becoming wet. Over the duration of the testing period, the gas pressure applied to the injection end of the clay sample and a pressure ramp was created to steadily increase the gas pressure, until the gas entry pressure was exceeded and gas entered the sample. The gas migrated through the clay and changes in porewater pressure, swelling pressure and flowrate were observed by the instrumentation around the sample. The porewater pressure showed a marked and almost instantaneous increase in pressure from about 1 MPa to about 10 MPa at 63.8 days, coinciding with a sudden spike in the outflow from the sample.

The data presented in this study shows that different recording instruments are required to provide a fuller picture of gas migration through bentonite because they show different features of the test at different times. The continued increase in the stresses measured by the axial and radial load cells after gas breakthrough mirrored the increase in injection pressure; this suggested that, at the start of the test, the sample was not in complete hydraulic equilibrium and a redistribution of the fluid in the sample caused the clay to continue to expand through the test

At day 71, the injection pump was stopped and the injection pressure was allowed to slowly decay. The outflow dropped to zero at this point, and no outflow was observed until day 81. After this point, the outflow was sporadic, occurring in fluctuations and spikes and suggesting that new gas pathways continued to open and close as the test progressed. The test has shown that there are dynamic processes were operating within the clay that will govern the spatial and temporal development of permeability within the sample.

References

British Geological Survey holds most of the references listed below, and copies may be obtained via the library service subject to copyright legislation (contact libuser@bgs.ac.uk for details). The library catalogue is available at: https://envirolib.apps.nerc.ac.uk/olibcgi.

ANGELI, M, SOLDAL, M, SKURTVEIT, E, and AKER, E. 2009. Experimental percolation of supercritical CO2 through a caprock. *Energy Procedia*, Vol. 1, 3351–3358.

HARRINGTON, J F, and HORSEMAN, S T. 1999. Gas transport properties of clays and mudrocks. 107–124 in *Muds And Mudstones: Physical And Fluid Flow Properties*. APLIN, A C, FLEET, A J, and MACQUAKER, J H S. (editors). Geological Society of London, Special Publication No. 158.

HARRINGTON, J F, NOY, S, HORSEMAN, S T, BIRCHALL, D J, and CHADWICK, R A. 2009. Laboratory Study of Gas and Water Flow in the Nordland Shale, Sleipner, North Sea. *AAPG Special Volumes*, DOI:10.1306/13171259St593394.

HARRINGTON, J. F. AND TAMAYO-MAS, E., 2016. Observational Evidence for the Differential Development of Porewater Pressure within Compact Bentonite and its Impact on Permeability and Swelling Pressure. BRITISH GEOLOGICAL SURVEY COMMERCIAL-IN-CONFIDENCE REPORT, CR-16-160.

HORSEMAN, S T, and HARRINGTON, J F. 1997. Study of gas migration in Mx80 buffer bentonite. *British Geological Survey Technical Report*, WE/97/7.

HORSEMAN, S T, HARRINGTON, J F and SELLIN, P. 2004. Water and gas flow in Mx80 bentonite buffer clay. 715–720 in *Symposium on the Scientific Basis for Nuclear Waste Management XXVII*. Materials Research Society (Kalmar) Volume 807.

HORSEMAN, S T, HIGGO, J J W, ALEXANDER, J, and HARRINGTON, J F. 1996. Water, gas and solute movement through argillaceous media. *NEA Report*, CC-96/1, OECD, Paris.

ORTIZ, L, VOLCKAERT, G and MALLANTS, D. 2002. Gas generation and migration in Boom Clay, a potential host rock formation for nuclear waste storage. *Engineering Geology*, Vol. 64 (2-3), 287–296.

WEETJENS, E, and SILLEN, X 2006. Gas generation and migration in the near field of a supercontainer-based disposal system for vitrified high-level radioactive waste. 1–8 in *Proceedings of the 11th International High-level Radioactive Waste Management Conference (IHLRWM), 30 April - 4 May 2006*. (Las Vegas, United States).

WIKRAMARATNA, R S, GOODFIELD, M, Rodwell, W R, Nash, P J, and AGG, P J. 1993. A preliminary assessment of gas migration from the Copper/Steel Canister. *SKB Technical Report*, TR-93-31.